PRELIMINARY ANALYSIS OF THE ATMOSPHERIC RADIATIVE HEATING FIELDS IN AUTUMN IN THE MID LATITUDE ARID AREAS OF CHINA

Ji Guoliang (季国良),

Lanzhou Institute of Plateau Atmospheric Physics, Academia Sinica, Lanzhou

K. N. Liou, S.C. Ou

Department of Meteorology, University of Utah, U.S.A.

and *M.D. Chou*

Laboratory for Atmospheres, NASA / Goddard Space Flight Center, U.S.A.

Received December 17, 1990

ABSTRACT

A parameterized radiation and cloud model developed at the University of Utah, U.S.A. has been used to compute the atmospheric radiative properties in Zhangye area during the pilot experiment of HEIFE in September of 1988. Some characteristics of atmospheric radiative heating fields during the autumn in Zhangye area have been analysed, and some questions that merit attention in the future observation are also discussed in this paper.

Key words: parameterized radiation and cloud model, radiation transfer, solar radiation heating rate, infrared cooling rate

I. INTRODUCTION

Recently, a great amount of studies have shown that the global temperature may arise and then the frequency of drought appearing may increase in the mid–latitude areas by the effect of the human activities and industrializations. Therefore, atmospheric scientists and environmental scientists both carry out a variety of activities in observation and research to monitor the global climate change. After the HAPEX (Hydrological–Atmospheric Pilot Experiment) and FIFE (First ISLSCP Field Experiment) of the ISLSCP (International Satellite Land–Surface Climatology Project) in WCRP (The World Climate Research Program), the HEIFE (Heihe Basin Field Experiment), supported by the National Natural Science Foundation of China, the Chinese Academy of Sciences and the Gansu Committee of Science and Technology, is carrying out by Lanzhou Institute of Plateau Atmospheric Physics and several other units. In order to study the characteristics of the air–land radiation budget and atmospheric heating fields, to provide effective radiation parameters for GCM and to monitor the surface climate change by satellite remote sensing data, based on the data observed in Zhangye and Huayin, Gansu Province in September of 1988, and through computation of radiation transfer program we analyse the characteristics of the atmospheric radiation heating fields in autumn of 1988 in Zhangye area, and discuss some questions interested to provide reference for the experiment that is implementing.

II. BRIEF DESCRIPTION OF PARAMETERIZED MODEL

The model used in this paper is an 18–layer model in σ–coordinates, that is a development of parameterized radiation and cloud program at the Department of Meteorology, University of Utah, U.S.A. (Ou and Liou, 1988). This model covers both infrared and solar bands of radiation. Utilizing the concepts of broadband emissivity, transmissivity and reflectivity, the problems of radiation transfer may be simplified and the computing time can be saved.

1. *Basic Equation Used in the Computation*

In a clear atmosphere, the upward and downward infrared fluxes at a given level may be written in the following forms(Liou, 1980):

$$F^{\uparrow}(u) = \sigma T_s^4\left[1-\varepsilon^f(u,\ T_s)\right] + \int_0^u \sigma T^4(u')K(u-u')du', \tag{1}$$

$$F^{\downarrow}(u) = \int_{u_1}^{u} \sigma T^4(u')K(u'-u)du', \tag{2}$$

where T_s is the surface temperature, u the path length of the absorbing gas, and u_l the total path length, ε and K the infrared broadband emissivity and Kernel function, respectively;

$$\varepsilon^f(u,\ T) = \int_0^{\infty} \pi B_v(T)\left[1-T_v^f(u)\right]dv/(\sigma T^4), \tag{3}$$

$$K(u-u') = -\frac{d}{du'}\varepsilon^f(\ |u-u'|,\ T(u')), \tag{4}$$

where T_v^f is the flux transmittance at the spectral wave number v, and πB_v the Planck flux.

In the program, the absorptions of water vapor, ozone and carbon dioxide are divided into five bands and an overlapping band, so that the broadband flux emissivity may be written in the form:

$$\varepsilon^f(u,\ T) = \sum_1^5 \varepsilon_i^f(\tilde{u}_i,\ T^f) + \varepsilon_6^f(\tilde{u}_w,\ \tilde{u}_c,\ T), \tag{5}$$

$$\varepsilon_i^f(\tilde{u}_i,\ T) = \exp(\sum_{n=0}^{3} C_{ni}\bar{u}_i^n), \tag{6}$$

$$\tilde{u}_i = (2\lg\bar{u}_i - \bar{a}_i)/\bar{b}_i, \tag{7}$$

where $\tilde{u}_i$ ($i=1$—6) denotes the individual absorbing path lengths with incorporated reduction of pressure and temperature effects, $\bar{a}_i$ and $\bar{b}_i$ are coefficients used for each band, and C_{ni} is obtained by the least square method.

In terms of the solar radiation transfer in a clear atmosphere, Rayleigh scattering due to air molecules is insignificant above a height z_l of about 10km. The downward and upward solar fluxes at level z above z_l may be expressed as

$$F^{\downarrow}(z) = \mu_0 S_0\left[1-A^{\downarrow}(z_T-z)\right], \tag{8}$$

$$F^{\uparrow}(z) = F^{\downarrow}(z_1)(r_a + G\vec{t}_a)\left[1-\vec{A}^{\uparrow}(z-z_1)\right],\quad z \geqslant z_1 \tag{9}$$

$$F^{\uparrow}(z) = F^{\downarrow}(z_1)\left[1 + \bar{A}^{\uparrow}(z_1 - z)\right], \quad z < z_1 \tag{10}$$

where z_T is the height of the top of the atmosphere, the solar constant S_0 is taken to be 1360W / m^2, r_a and t_a represent the reflectivity and transmissivity of Rayleigh scattering respectively, and G is a non–dimensional upward diffuse component at the surface involving multiple reflections between the Rayleigh scattering layer and the surface with a Labertain albedo of r_s,

$$G = t_a r_a \left(1 - \bar{r}_a r_s \cdot \bar{t}_a^2\right)^{-1}. \tag{11}$$

The solar absorptivities for water vapor, ozone and carbon dioxide may be expressed in the following form:

$$A(z) = \sum_i A_i(u_o / \mu_0)f_i + \sum_i A_i(u_w / \mu_o)f_i + \varepsilon A_s(u_c / \mu_o), \tag{12}$$

where u_o, u_w and u_c represent respectively the path lengths for O_3, H_2O, and CO_2, and f_i is the fractional solar flux associated with the individual bands of absorptivity A_i, ε is the H_2O–CO_2 overlapping correction at the 2.7μm band. The parameterized expressions of the absorptivities for the three absorbers are documented in Liou and Ou(1981; 1983).

2. *Computation of the Model in Cloudy Atmosphere*

In this program, our major emphasis is on the development of accurate and stable radiation programs for atmospheres with even three–layer clouds, i.e., containing high, middle and low clouds, on the basis of two–layer cloud system considered previously (Liou et al., 1984). First, it is assumed the high, middle and low cloud decks to fill, respectively, 5—9 layers, 10—12 layers and 13—15 layers, and in vertical , the cloud is assumed to fill the whole deck domain, i.e., the cloud top is at the top of the highest model layer in the deck and the cloud base is at the bottom of the lowest model layer in the deck. Second, available cloud cover prediction schemes used Geleyn's specification of h_c,

$$h_c = 1 - \alpha\sigma(1 - \sigma)\left[1 + \beta(\sigma - \frac{1}{2})\right], \tag{13}$$

where $\alpha = 2$, $\beta = \sqrt{3}$, $\sigma = p / p^*$ and p^* is the surface pressure. Third, in this program, the total cloud cover for each horizontal grid space has used the maximum schemes, i.e., the total cloud cover is taken the maximum among the high, middle and low cloud covers, respectively. Moreover, this program uses the maximum overlapping assumption when the high, middle and low clouds appear simultaneously. In each partially cloudy grid space, the total cloud fraction $n = \max(n_l, n_m, n_h)$ and the clear fraction is $(1-n)$. The program also sets $n = n_l = n_m = n_h$ for the sake of saving computer time, whenever $n_l, n_m, n_h > 0$. If, however, the total cloud cover is greater than 0.9 (or less than 0.1), the grid is counted as completely overcast (clear).

When we calculated the infrared radiation, the high cloud deck is considered to be non–black, both middle and low clouds are considered to be blackbodies. Then, the broadband infrared emissivity, transmissivity and reflectivity for high clouds are the functions of the vertical cloud liquid water content:

$$R(W)=\sum_{i=0}^{5} C_i W^i \ . \tag{14}$$

And the broadband solar reflectivity and transmissivity may be expressed in the following form:

$$r,\ t(\mu_0,\ W)=\sum_{m=0}^{3}\sum_{n=0}^{3} b_{mn}\mu_0^m W^n \ . \tag{15}$$

The coefficients C_i and b_{mn} in the above equations are given in Liou and Wittman (1979).

III. CALCULATED RESULTS AND DISCUSSIONS

In the computation, the routine surface meteorological data and atmospheric stratification from rawinsondes are taken from Zhangye Station(38°50′N, 100°26′E, 1483m A.S.L.), Gansu Province, during Sept. 1—20, 1988. The surface albedo is set to be 0.20, and the cosine value of solar zenith angle is set to be 0.20 both in the morning and evening. The sky is clear or cloudy, and no wind and no larger precipitation processes occur, and the variable range of surface albedo is less than 5% during the whole period of calculation.

In clear atmosphere, the computed results are compared with the observations (Ji, 1990). It is shown that for the surface net solar radiation, the mean relative error of the computation is 7.0% and the mean square error 5.0%; and for the atmospheric downward IR flux, the mean relative error 8.0% and mean square error 3.8%. Obviously, the errors are larger in this paper than those of Cai (1987) dealing with the QXPMEX in 1979. The main causes may be as follows: First, there are fewer data in the clear atmosphere and the radiosounding data are only obtained in the morning and evening, therefore the errors become larger because the tilted solar rays in the morning and evening has a longer path passing through the atmospheric boundary layer. Second, the observational data used in comparison are 30–minute average values, thus the error becomes larger in the morning and evening because the solar zenith angle changes very fast in that time. Third, the data used in comparison are the instantaneous ones from Huayin(39°09′N, 100°08′E, 1450m A.S.L.) with the gravel underlying surface, which is 30—40km from away Zhangye so that the large errors may also be caused by the mismatch of time and space of the radiosonde measurements and surface observations. In addition, no considering the effects of aerosol on radiation may lead the computed results to be rather larger than the measured.

Table 1. The Irradiance (in W / m^2) in Clear Atmosphere at Zhangye (Sept. 1—20, 1988)

Time (BT)	TOP			Surface			
	solar flux	IR flux	net radiation	net solar flux	net IR flux	net radiation	total downward IR flux
0800	208	241	−33	145(134)	86(84)	59	255(290)
2000	208	269	−61	146(136)	115(100)	31	286(299)
1200	850	343	507	689(678)	366(349)	323	292(287)

Note: Data in parenthese refer to observation.

The relative errors are rather smaller in the stable cloudy atmosphere than in the clear atmosphere. The mean error is 3.4% and the mean square error is 2.4% for the surface net solar radiation, and the mean error 7.3% and mean square error 9.1% for the atmospheric downward IR flux.

Therefore, the model is available to compute the energy budget in the air–land system in Zhangye area.

The characteristics of the atmospheric radiative heating fields in Zhangye area in the fall of 1988 will be discussed in the following.

1. *Characteristics of the Atmospheric Radiative Heating Fields in Zhangye Area*

(1) *In the clear atmosphere*

The air–land average radiation budget of four clear days during the first 20 days in September of 1988 is shown in Table 1.

1) Because the solar zenith angle is nearly the same in the morning (0800BT) as in the evening (2000BT), the solar radiation flux on TOP (the top of the atmosphere hereafter) and the net solar radiation flux at the earth's surface are almost the same. However, the surface temperature is rather higher in the evening than in the morning, and the case is true with the moisture in the atmosphere, for those reasons, the IR flux on TOP, IR flux at the surface and the atmospheric downward IR flux are all larger in the evening than in the morning, i.e., the radiative cooling of the atmosphere and the ground is stronger in the evening than in the morning. The less downward IR and the larger surface net IR fluxes calculated show that the precipitable water is small and the air temperature is low in this area (Wu, 1989), of which the characteristics have a close relation to the semi–arid climate.

2) At noon, the radiative heating is very strong in Zhangye area, and the net radiations on TOP and at the surface may reach 507W / m^2 and 323W / m^2, respectively.

The solar heating rate and the IR cooling rate in the clear atmosphere are shown in Table 2, from which we can see that:

1) The maximum solar heating rate is on TOP and the heating rates at the other layers are less than 1.0K / d. Near the surface the heating rate is 0.74K / d in the morning and 0.78K / d in the evening, and it may be up to 3.2K / d at noon.

2) The maximum IR cooling rate appears near the surface, with the value −8.8K / d in the morning and up to −14.7K / d in the evening. So far as the troposphere is concerned, the IR cooling rate ranges between −1—−3K / d in both morning and evening. The strong cooling in the morning and evening and the sharp heating at noon produce the large diurnal temperature difference. This is a significant climatological characteristic in the arid area, which will contribute to the accumulation of organic matter in the plant.

Table 2. The Maximum Average Heating Rate H_s, the Cooling Rate H_l and the Net Heating Rate H_n near the Surface in the Clear Atmosphere in Zhangye (Sept. 1—20, 1988) (in K / d)

Time (BT)	H_s	H_l	H_n
0800	0.74	−8.83	−8.09
2000	0.78	−14.68	−13.90

These results are compared with those in Lhasa(29°42′N, 91°48′E) in the Qinghai–Xizang

Plateau in September of 1982. It can be seen that the solar radiative heating rate near the surface is larger in Lhasa (above 1.0K / d) than in Zhangye in either morning or evening, and the IR cooling rate is also larger in Lhasa(−17.4K / d) than in Zhangye. It is clear that once entering autumn the rapid cooling near the surface will make the atmospheric heating fields change from heat source to heat sink over the whole Plateau(Ji, 1989), but this transformation is late and slow in Zhangye area.

(2) *In the cloud atmosphere*

The radiative energy budget in the air–land system calculated from this model for various cloudy atmospheres is shown in Table 3, from which we can see that:

1) When there are 10 tenths of high cloud in the sky, for instance, at 0800BT 15 September, the solar flux is 182W / m^2 and the IR flux is 226W / m^2 on TOP, the net solar flux is 118W / m^2 at the surface, the surface net IR flux is 91W / m^2 and atmospheric downward IR flux is 267W / m^2.

2) When there are 10 tenths of middle cloud or middle and low clouds in the sky, e.g., in the case of Sept.11 and 12, the net solar flux at the surface is only 4—5W / m^2 because of the weak transmission through the middle and low clouds, while the atmospheric downward IR flux is large, about 360W / m^2, so that the surface net IR flux can be very small, about 20W / m^2.

Table 3. The Solar Radiation Flux (in W / m^2) in the Cloudy Atmosphere

Time (BT) h / d / m	Cloud amount	Cloud type	TOP			Surface			
			solar flux	IR flux	net radiation	net solar flux	net IR flux	net radiation	total downward IR flux
0800 / 11 / 9	10	Ac Ci	78	184	−105	4(17)	20(42)	−16	363(356)
0800 / 12 / 9	10	Ac As	76	188	−111	5	24	−18	362
0800 / 15 / 9	10^-	Ci	182	226	−43	118(120)	91(55)	27	297(350)
0800 / 16 / 9	10^-	Ci Ac	77	179	−102	4	8	−3	347

Note: Data in parenthese refer to observations.

3) When there are 10 tenths of high and middle clouds in the sky (such as on Sept. 16), the situation is the same as that with 10 tenths of high, middle and low clouds. The net radiation flux of the air–land system is about −100W / m^2, and the net solar flux and the net IR flux at the surface are very small.

In addition, it is shown from the calculated results that when low clouds, including one deck low cloud, or two decks of middle and low clouds or high and low clouds, or three decks of high, middle and low clouds, exist in the sky, the atmospheric downward IR flux reaches the maximum of 360—370 W / m^2, and the surface IR flux may be a negative value, which is consistent with Weng(1979).

The solar heating rate and the IR cooling rate in various cloud types are shown in Figs.1 and 2 which indicate that:

1) In the case of one deck of high cloud in the sky, the solar heating rate in the cloud body can reach the maximum (such as 0.7K / d) and the IR cooling rate ranges between −1— −2K / d.

2) In the case of one deck of middle cloud in the sky, the solar heating rate near 500hPa

level is 1.5K / d and rather small at the other layers. While in mid–cloud domain there is a maximal IR cooling rate of −13 to −14K / d, under this domain exist some no heating and positive heating levels.

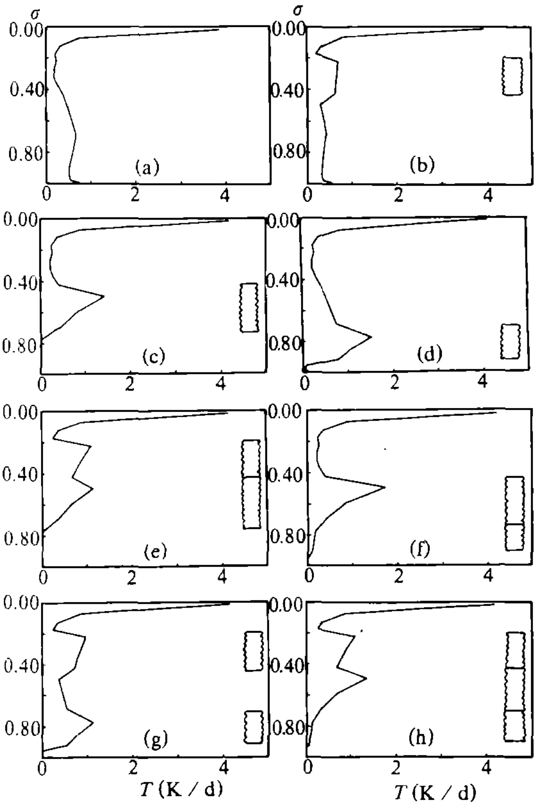

Fig. 1. The solar heating rate in weather situations in Zhangye in Sept. 1988: a. clear, b. high cloud, c. middle cloud, d. low cloud, e.high and middle cloud, f. middle and low cloud, g. high and low cloud, h. high, middle and low cloud.

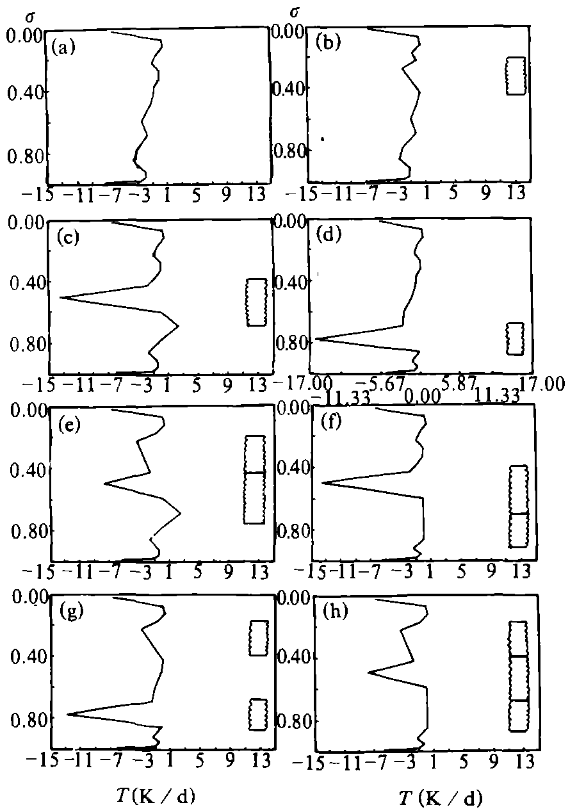

Fig. 2 As in Fig.1 but for the infrared cooling rate.

3) In the case of one deck of low cloud, the solar heating is about 1.5K / d and the maximum IR cooling rate is −16K / d which is larger than the calculated result with the data of 1962 U.S. Standard Atmosphere(Ou and Liou, 1988). It thus can be seen that the IR cooling is very strong in atmosphere above Zhangye in autumn and smaller near the surface than the other levels.

4) In the case of two decks of cloud, discussion will be on the following situations: with high and middle clouds, the solar heatinng rate is the same as that with high, middle and low clouds, and its maximum appears in 200—500hPa, with the order of 1K / d. But the heating rate is rather small under the low cloud. The maximal IR cooling rate appears in the middle cloud region reaching −8K / d near 420hPa under which occur no cooling and positive heating

layers; with middle and low clouds, the solar heating rate reaches a maximum of 1.7K / d in the layer of 400—500hPa, and the IR cooling rate reaches a maximum of −13.7K / d near 420hPa under which exist the four layers with zero cooling rate. The IR cooling rate is about −6K / d near the surface similar to that with one deck of low cloud. With high and low clouds presented in the sky, the solar heating rate is maximum with the value of 1K / d in the high cloud region and 1.1K / d in the low cloud region. The heating rate is rather small near the surface. The IR cooling rate increases in the high cloud region and the maximum IR cooling rate of −13K / d appears in the low cloud region.

Table 4. The Average Values of Daily Radiance in Zhangye in Sept. 1—20, 1988 (in W / m^2)

Time	Item	total cloud amount	TOP net solar flux	TOP net IR flux	TOP net radiation	surface net solar flux	surface net IR flux	total flux downward	surface net radiation
0800BT	1st decade	0.3	170	227	−57	101	65	289	36
	2nd decade	0.8	105	192	−87	32	27	328	4
	3rd decade	0.5	144	212	−68	74	51	305	23
2000BT	1st decade	0.5	144	224	−79	74	71	343	3
	2nd decade	0.5	144	221	−77	74	68	333	6
	3rd decade	0.5	144	222	−78	74	70	338	4

(3) *In the Average Conditions*

The 10–day average data are used to calculate the first and second 10–day and the 20–day average in September of 1988. Table 4 shows the average values of the components of radiation in the air–land system of Zhangye area in September of 1988. It can be seen that:

1) In the first 10 days, 3 tenths of cloud cover in the sky made the net solar flux on TOP and at the surface both larger than that in the second 10 days, and the IR flux is smaller, which cause the net radiation flux of the air–land system and the surface to be larger in the first 10 days.

2) In the first 10 days, the cloud cover is more in the evening than in the morning, so the net solar fluxes on TOP and at the surface are both smaller than those in the morning, the net IR flux in the morning is close to that in the evening, and the atmospheric downward IR flux is obviously larger in the evening than in the morning; In the second 10 days, the net solar fluxes on TOP and at the surface both are smaller in the morning than in the evening because of the fewer cloud cover in the evening. The net IR flux is still larger in the evening, which may be caused by the more moisture and the higher surface temperature in the evening than in the morning.

3) In terms of the average situation during 1—20 of September, the total cloud covers in the sky are equal in both morning and evening, so their solar fluxes are close as well, but the net IR flux is larger in the evening than in the morning.

It is shown in Figs.3 and 4 that in the morning, the solar heating rate is larger in the second than the first ten days because in the morning there mainly exist high and middle clouds in the sky. The solar heating rate is 0.9K / d in the second 10 days and 0.5K / d in the first in the high cloud region. The IR cooling rate is larger in the second than the first 10 days, and the maximal is −7K / d in the second and −3.4K / d in the first 10 days in the middle cloud region, and the maximal IR cooling rate appears near the surface about −5.4K / d. For the net atmospheric hea ting rate, the maximal cooling rate of about −6K / d appears at about 420hPa level in the second 10 days. In the first ten days, the maximal cooling rate about −4.9K / d appears near the surface. In the evening, the solar heating rate and the IR cooling rate both are consistent in midd le and high cloud regions and the maximum values are 0.6K / d and −4.8— −4.9K / d, respectively. Near the surface, the IR cooling rate is −10—−11K / d in the first twenty days.

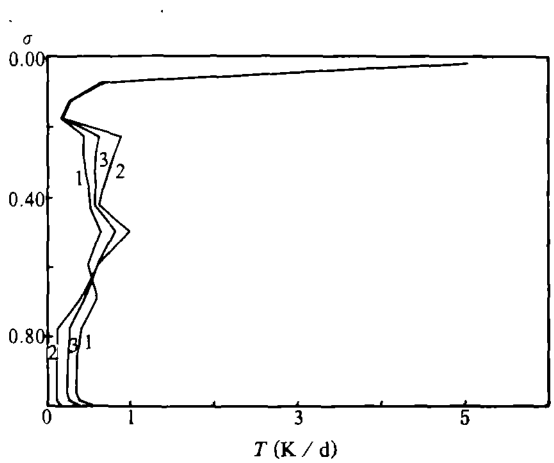

Fig. 3. Average solar heating rate for Sept. 1—20, 1988.

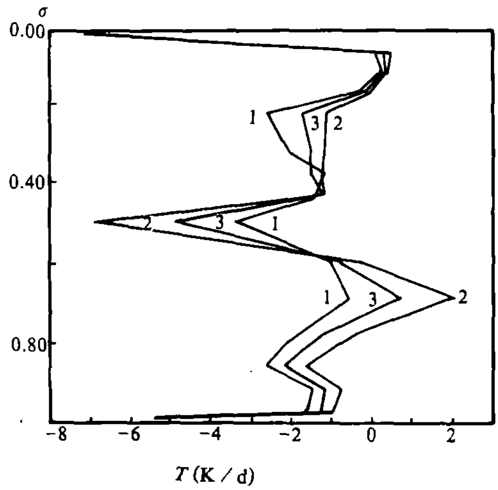

Fig. 4 The same as in Fig.3, but for IR cooling rate.

2. *Discussion on Some Factors Affecting Radiation*

(1) *The solar zenith angle*

Table 5 shows the calculated results versus C_z, the cosine values of solar zenith angle on 14 Sept., 1988. It can be seen that with the solar zenith angle, the IR flux does not change, but the solar radiation changes obviously. For example, taking $C_2 = 0.1$, the net solar flux on TOP and at the surface is 96 and 58W / m^2, respectively. The difference may be great at the different solar zenith angles. So it is obviously that the solar zenith angle plays a significant role on the solar radiation flux.

Table 5. The Irradiance at the Different Solar Zenith Angles ($A = 0.25$)

C_z	TOP net solar flux	TOP net IR flux	TOP net radiation	surface net solar flux	surface net IR flux	surface net radiation	total downward IR flux
0.1	96	248	−152	58	83	−25	257
0.2	200	248	−48	136	83	53	257
0.3	306	248	57	220	83	137	257
0.4	414	248	165	307	83	224	257

It is will known that the variation of the solar zenith angle is very fast in the morning and evening, for example, in Zhangye from 0730—0830BT on Sept. 14, 1988, the solar zenith angle changes from 85.7°to 74.0°, and C_z changes from 0.07 to 0.27. Obviously, the sampling time will affect greatly the observational data, thus it must be imposed on great attention.

(2) *The surface albedo*

Fig.5 shows the curves of solar heating rate in various surface albedos. It is found that:

1) The solar flux and the net radiation flux on TOP and at the surface decrease linearly and the IR flux does not change with the increase of the surface albedo.

2) The surface albedo change affects the solar heating rate only in the lower atmosphere, i.e., with the surface albedo increasing, the solar heating rate increases in the lower atmosphere, but does not change in the higher. The IR cooling rate does not change with the surface albedo.

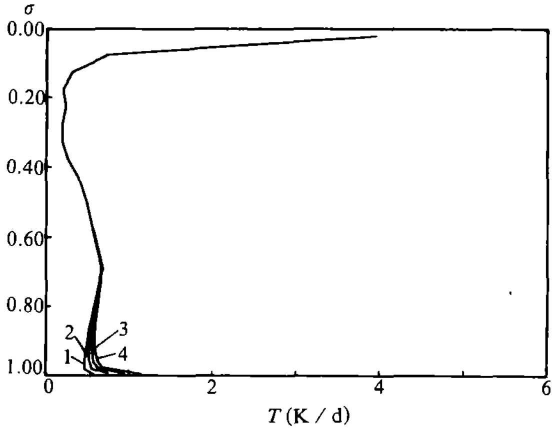

Fig. 5. The solar heating rate in various surface albedos. 1. A = 0.10, 2. A = 0.20, 3. A = 0.30, 4. A = 0.40.

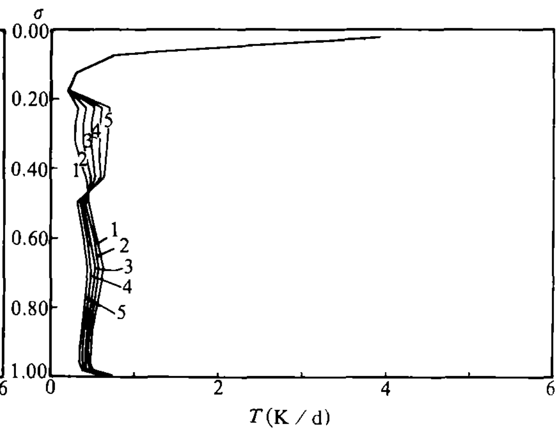

Fig. 6. The solar heating rate in various cloud amount of high cloud. 1. $n = 0.2$, 2. $n = 0.4$, 3. $n = 0.6$, 4. $n = 0.8$, 5. $n = 1.0$.

(3) *The total cloud cover in the sky*

The radiation flux with various total cloud covers of seven cloud types has been calculated:

1) When the total cloud cover is 1 tenth and 9 tenths, the results are similar to those of the clear and the overcast days respectively, i.e., with 1 tenth and 9 tenths of cloud, the results can be dealt with as the clear and overcast models, respectively.

2) When one deck of high cloud exists in the sky, the downward IR flux is not very sensitive to the variance of cloud cover, and has a variation range only about 5—6W / m^2. But with one deck of low cloud appearing in the sky, the downward IR flux is very sensitive to the variance of cloud cover, and the variation range can reach 80—100W / m^2. The above results are consistent with Wu(1989). Our experiments also show that with one deck of middle cloud appearing in the sky, the decrease in the solar flux with increasing total cloud cover would be maximal and that the downward IR flux increases greatly with increasing low cloud cover.

3) In the case when both high and middle clouds are present, the changes of all sorts of radiation fluxes with the total cloud cover are the same as those of one deck of middle cloud. In

the case of both middle and low clouds presented, the situations are also like that with middle cloud. In the case of high and low clouds, the total cloud cover affects radiation fluxes as one deck of low cloud does.

4) In clouds, the solar heating rate increases with the increase of cloud cover (see Fig.6) but below clouds it decreases with increasing total cloud cover because of fewer transmissive flux through more cloud cover. So does the IR flux. The above results are consistent with Liou(1989).

From above discussions, it can be seen that different cloud heights and cloud covers in the model may yield large difference of calculation. So it is necessary to select more objective cloud height and cloud cover, and this will require more for the cloud parameter observations.

(4) *The surface temperature*

It is found from calculation that the surface temperature plays an important role in the model. In this model , the surface temperature from extrapolation formula is close to the observations in the morning and evening, but significantly lower in the other daytime. In addition, the calculation also indicates that because the surface temperature is lower than the air temperature in the morning and evening, the surface IR upward flux calculated by using the observed surface temperature is lower than the observed in both morning and evening, but the calculated is higher than the observed in the other daytime. Thus it is necessary to make correction on the surface temperature in the calculation(Cai,1987). In such an arid area of Zhangye, for lack of ideal pilot experiment data, how to make corrections on surface temperature needs to be further explored to find an available method. Similarly, attention must be paid to the effect of surface emissivity on radiation.

In addition, it is also found that the solar flux seems not very sensitive to the change of moisture, which is consistent with Pinker(1985).

IV CONCLUSIONS

(1) The model is available to the radiation parameterization calculation in the mid–latitude arid regions of China.

(2) At autumn noon of Zhangye area, solar radiative heating is strong, and in the morning and evening, especially in the evening, the IR cooling is very strong, which produces the obvious diurnal air temperature difference. Meanwhile, the strong atmospheric cooling accelerates the seasonal transition from summer to winter of the radiative heating fields in this area.

(3) The amount of middle cloud affects mostly solar radiation and that of low cloud affects greatly the atmospheric downward IR radiation.

(4) The changes of the surface albedo and the solar zenith angle have obvious influences on the solar radiation, and the cloud height and cover do greatly influences on both the solar and IR radiations. Therefore these parameters should be selected carefully in observation and computation. The water content in the cloud affects largely the solar radiation, so it is essential to be selected carefully in the arid region. The surface temperature is also an important parameter in this model and the correction of it should be further explored and improved.

The subject of HEIFE is supported by the National Natural Science Foundation of China, the Chinese Academy of Sciences and the Gansu Committee of Science and Technology. This work is conducted at the Department of Meteorology, University of Utah, U.S.A. and supported by NASA climate program managed by Dr. Robert Schiffer.

REFERENCES

Cai Qiming et al. (1987), Model calculation of radiative properties in the Qinghai–Xizang Plateau atmosphere, Atmospheric Radiation Progress and Prospects, Proceedings of the Beijing International Radiation Symposium, Beijing, China, August 26—30, 1986, pp.107—115.

Ji Guoliang and Pu Ming (1989), Characteristics of the surface and atmospheric heating fields over Qinghai–Xizang Plateau for the period from August 1982 to July 1983, *Acta Meteorologica Sinica*, **3**:228—241.

Ji Guoliang et al. (1990), A preliminary analysis of the solar radiation condition in Zhangye area during September 1988, *Plateau Meteorology*, **9**:194—201 (in Chinese).

Liou, K.N. and Wittman, G.D. (1979), Parameterization of the radiative properties of clouds, *J. Atmos. Sci.*, **36**:1261—1273.

Liou, K.N. (1980), *An Introduction to Atmospheric Radiation*, Academic Press, pp.392.

Liou, K.N. and Ou, S.C. (1981), Parameterization of infrared radiative transfer in cloudy atmospheres, *J. Atmos. Sci.*, **38**:2707—2716.

Liou, K.N. and Ou, S.C. (1983), Theory of equilibrium temperature in radiative–turbulent atmospheres, *J. Atmos. Sci.*, **40**:214—229.

Liou, K.N., Ou, S.C., Kinne, S. and Koening, G. (1984), Radiation parameterization programs for use in general circulation models, AFGL–TR–84–0217.

Liu, Chungming and Ou, S.C. (1989), The numerical study of cloud effect on atmospheric radiation, *Atmospheric Sciences(Taipei)*, **16**:409—434 (in Chinese).

Ou, S.C. and Liou, K. N. (1988), Development of radiation and cloud parameterization programs for AFGL global models, AFGL–TR–88–0018.

Pinker, R. T. and Ewing, J. A. (1985), Modeling of surface solar radiation: model formulation and validation, *J. Clim. Appl. Meteor.*, **24**:389—401.

Weng Duming et al. (1979), The radiation conditions at Kunlun Pass, *Journal of Nanjing Institute of Meteorology*, **3(1)**:11—19 (in Chinese).

Wu, M. L. and Cheng Chee–Pong (1989), Surface downward flux computed by using geophysical parameters derived from HIRS 2 / MSU soundings, *Theor. Appl. Climatol.*, **40**:37—51.